ChemComm

COMMUNICATION

View Article Online
View Journal | View Issue

A facile method for the synthesis of the $Li_{0.3}La_{0.57}TiO_3$ solid state electrolyte†

Cite this: *Chem. Commun.*, 2014, **50**, 5593

Received 15th January 2014,
Accepted 30th March 2014

DOI: 10.1039/c4cc00335g

www.rsc.org/chemcomm

Qifeng Zhang,[a] Nick Schmidt,[a] Jolin Lan,[a] Whungwhoe Kim[b] and Guozhong Cao*[a]

We report a facile method for the synthesis of $Li_{0.3}La_{0.57}TiO_3$ by forming a coagulated precursor solution which contains Li^+, La^{3+}, and TiO_2 nanoparticles mixed highly homogeneously. The grain and overall conductivities of the synthesized $Li_{0.3}La_{0.57}TiO_3$ are comparable to the values in literature for the material prepared by other methods.

There has been an increasing demand for solid state electrolytes for use in lithium batteries to replace the currently widely used liquid electrolytes in recent years. Compared to liquid electrolytes, solid state electrolytes possess the advantages of providing lithium batteries with much safer operation[1,2] and making the manufacture easier thus resulting in significant reduction of battery cost. In some cases, use of solid state electrolytes has become an essential requirement. For instance, in lithium ion batteries, solid state electrolytes have been expected to replace the liquid electrolytes with the consideration of blocking the growth of lithium dendrites through charge–discharge cycles; such lithium dendrites may connect the anode and the cathode ultimately causing an internal short circuit of the battery.[3–5] Solid state electrolytes are also desired for lithium–air battery applications, where they serve as membranes to separate the organic electrolyte from the aqueous electrolyte. The organic electrolyte is adopted to protect the lithium anode from reacting with water, while the aqueous electrolyte is used to facilitate the dissolution of lithium oxides (particularly lithium peroxide, Li_2O_2) formed at the cathode during discharge, which are insoluble in organic electrolytes and may therefore cause either passivation or pore blocking of the cathode, which is typically made of porous carbon.[6,7] In addition, solid state electrolytes are also integral components for the construction of lithium batteries to operate at temperatures below −10 °C or above 60 °C, which are the temperature limits for most liquid electrolytes.[8]

Many efforts have been made to develop solid state electrolytes, including the use of both inorganic materials and polymers.[9–11] The advantage of polymer-based electrolytes is that they are bendable and therefore can work with flexible substrates and are compatible with the roll-to-roll technology. However, the polymer-based electrolytes suffer from poor chemical stability especially when taking into account the heat generation, which occurs during the battery operation. Compared to polymer-based electrolytes, inorganic electrolytes demonstrate much better chemical stability and, more importantly, present significantly higher lithium ionic conductivity, typically on the order of 10^{-5}–10^{-3} S cm^{-1}, compared to 10^{-8}–10^{-6} S cm^{-1} for most polymer electrolytes.[12–14] Among the existing inorganic electrolytes, lithium lanthanum titanate (LLTO) has been identified as the most promising one in view of its high lithium ionic conductivity, typically on the order of 10^{-4}–10^{-3} S cm^{-1} (for single crystalline grains).[10,15–18] Such a conductivity level is averagely higher than that for Na super-ionic conductor-type phosphate, which is another inorganic solid state electrolyte with great potential,[10,19–21] and is apparently 1–2 orders of magnitude higher than the conductivities of other inorganic solid electrolytes, such as 10^{-6}–10^{-4} S cm^{-1} for garnet structure materials,[22–24] and 10^{-5}–10^{-3} S cm^{-1} for Li_2S-based oxysulfide glasses.[25,26] In addition to the advantage of having high conductivity, good thermal stability and the use of nontoxic elements are also amongst the merits of lithium lanthanum titanate over other inorganic solid state electrolytes.

Lithium lanthanum titanate is a ceramic material possessing ABO_3 perovskite structure, in which A represents Li and La, and B represents Ti, forming a lithium–lanthanum–titanium oxide with the formula of $Li_{3x}La_{2/3-x}TiO_3$ ($0.21 \leq 3x \leq 0.50$). In lithium lanthanum titanate, the migration of lithium ions is based on a hopping process, through which the lithium ions move in a three-dimensional network of vacancy defects located at A sites. Lithium ion conduction within lithium lanthanum titanate is very sensitive to the concentration of lithium, in other words, the stoichiometric ratios of the Li^+ to La^{3+} and TiO_3^{2+}. It has been found that $Li_{3x}La_{2/3-x}TiO_3$ in the case of x = 0.1, *i.e.*, $Li_{0.3}La_{0.57}TiO_3$, may give the highest lithium ionic conductivity, which is generally on the order of 10^{-4}–10^{-3} S cm^{-1}. However, the performance of $Li_{0.3}La_{0.57}TiO_3$ for lithium ion

[a] *Department of Materials Science and Engineering, University of Washington, Seattle, WA 98195, USA. E-mail: gzcao@u.washington.edu*
[b] *Nuclear Application Tech. Development Department, Korea Atomic Energy Research Institute, Daejeon, 305-353 Republic of Korea*

† Electronic supplementary information (ESI) available: TGA result, Fig. S1. See DOI: 10.1039/c4cc00335g

conduction is largely dependent on the method of synthesis, which affects the $Li_{0.3}La_{0.57}TiO_3$ in terms of its composition, the morphology, structure, surface chemistry and crystallinity of individual grains, as well as grain boundaries. In literature, $Li_{0.3}La_{0.57}TiO_3$ has been reported to be synthesized using either a solid state reaction method or a sol–gel based method. However, the solid state reaction method usually requires the use of ball milling,[15,27–29] *i.e.*, a mechanical way, to achieve better mixing of the starting materials which are in the form of powder containing Li^+, La^{3+} and Ti^{4+}. This, on one hand, makes the material processing time consuming and, on the other hand, is not an effective way to achieve a perfectly homogeneous dispersion of the starting materials, thus resulting in the existence of impure $Li_{0.3}La_{0.57}TiO_3$ in the final product. The impure $Li_{0.3}La_{0.57}TiO_3$ has the composition deviating from the stoichiometric one and accordingly yields unsatisfactory reproducibility of the lithium ion conduction performance of the final product.[28,29] The sol–gel method may solve the homogeneity problem in the solid state reaction method to some extent, but it is also unfavorable because of the lack of extensibility of a sol–gel method when considering stringent conditions for the formation of a $Li_{0.3}La_{0.57}TiO_3$ sol and the need for using rare or expensive chemicals, which serve as solvents and/or surfactants to form and stabilize the sol, leading to a high cost of material synthesis.[30–33] Herein, we report a facile method, *i.e.*, the so-called coagulated solution method in this communication, for the fabrication of $Li_{0.3}La_{0.57}TiO_3$. This method is relatively simple, low-cost, solution-based, and can produce a precursor powder containing the starting materials Li, La and Ti (or TiO_2) efficiently with good homogeneity, thus to a large extent overcoming the drawbacks of the solid state reaction method such as the difficulty in getting ideally mixed starting materials and the sol gel method, which is complicated and of high cost. The $Li_{0.3}La_{0.57}TiO_3$ synthesized using our method demonstrates a decent lithium ionic conductivity on the order of 10^{-4} S cm^{-1} for single crystalline grains of the lithium lanthanum titanate and an overall conductivity on the order of 10^{-5} S cm^{-1}, the latter else counts the resistance arising from grain boundaries in view of the polycrystalline structure of the bulk lithium lanthanum titanate material. Such an overall conductivity on the order of 10^{-5} S cm^{-1} is comparable to or at a slightly higher level compared with the values in literature for the $Li_{0.3}La_{0.57}TiO_3$ synthesized using a solid state reaction method or a sol–gel method, which varies in a wide range, from 10^{-6} S cm^{-1} to 10^{-4} S cm^{-1}, relying on the material microstructure, processing parameters, and measurement conditions.[29,34–36]

In a typical synthesis, 0.02 mol of lithium acetate dihydrate ($LiAc{\cdot}2H_2O$) was firstly dissolved in 200 mL of acetic acid (HAc). After $LiAc{\cdot}2H_2O$ has been dissolved completely, 0.067 mol of TiO_2 in the form of nanoparticle powder (P25, commercial TiO_2 nanoparticles, Sigma Aldrich) was added, and then the as-obtained mixture was stirred for several hours to enable the TiO_2 nanoparticles to fully disperse, resulting in the formation of a uniform dispersion of TiO_2 nanoparticles in HAc containing $LiAc{\cdot}2H_2O$. 0.0385 mol of lanthanum acetate hydrate ($LaAc_3{\cdot}1.5H_2O$) was then added to this dispersion. After approximately 20 min of vigorous stirring, the liquid dispersion turned into a white coagulated solution, resulting in the formation of a quasi-solid system which consists of Li^+, La^{3+}, and TiO_2 nanoparticles dispersed homogenously. The molar amounts adopted here

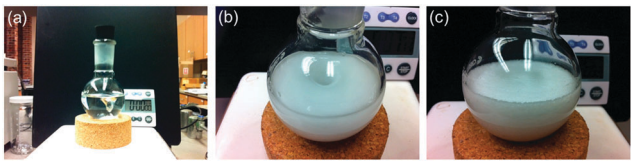

Fig. 1 A record of the transition of a dispersion containing $LiAc{\cdot}2H_2O$, $LaAc_3{\cdot}1.5H_2O$, and TiO_2 nanoparticles in HAc from a liquid to a coagulated solution. (a) A clear solution of $LiAc{\cdot}2H_2O$ in HAc, (b) TiO_2 nanoparticles and $LaAc_3{\cdot}1.5H_2O$ were added to the solution of $LiAc{\cdot}2H_2O$ in HAc, and (c) a coagulated solution forms after being stirred for ~20 min.

for $LiAc{\cdot}2H_2O$, $LaAc_3{\cdot}1.5H_2O$, and TiO_2 are to obtain $Li_{0.3}La_{0.57}TiO_3$ with stoichiometric ratios, *i.e.*, Li : La : Ti : O = 0.3 : 0.57 : 1 : 2. Fig. 1 shows a progression of the transition of the liquid dispersion to a coagulated solution as the $LiAc{\cdot}2H_2O$, TiO_2 nanoparticles and $LaAc_3{\cdot}1.5H_2O$ were sequentially added into the HAc solvent. The coagulated solution was then subjected to freeze drying to remove the HAc solvent, resulting in the formation of a dry precursor powder which contains all necessary components: Li^+, La^{3+}, and TiO_2 for the synthesis of lithium lanthanum titanate. Note that the conversion of the liquid precursor into a coagulated solution is a key feature of our method, which makes the positions of the Li^+, La^{3+}, and TiO_2 spatially fixed during the consequential freeze drying treatment and as a result the distribution of all component elements remains highly homogenous when the dry precursor powder forms. It is anticipated that a homogenous component element distribution may facilitate achieving high quality $Li_{0.3}La_{0.57}TiO_3$ by avoiding local composition deviations from the stoichiometry. The formation of a coagulated solution is speculated to originate from the common ion effect[37] in view of the fact that acetic acid was used as solvent for the dissolution of $LaAc_3{\cdot}1.5H_2O$ and $LiAc{\cdot}2H_2O$, but the specific mechanism in regard to such an experimental observation still needs to be explored further.

Before being made into pellets, the freeze dried precursor powder was pre-treated by heating at 750 °C with the aim of getting rid of the crystallization water from the $LiAc{\cdot}2H_2O$ and $LaAc_3{\cdot}1.5H_2O$ and also getting the lithium and lanthanum acetates to further decompose to oxides, so as to avoid a big volume change when the pellets were sintered. The reason for adopting 750 °C is based on the thermogravimetric analysis (TGA) as shown in Fig. S1 (ESI†), revealing that the elimination of crystallization water occurs at the temperature around 100 °C, corresponding to the 1st weight loss, and the decomposition of lithium and lanthanum acetates takes place in the temperature range from ~250 °C to ~700 °C, resulting in the 2nd and 3rd weight losses.

Shown in Fig. 2 are XRD patterns of the freeze dried powder (Fig. 2a) and the powder annealed at elevated temperatures (Fig. 2b–d), exhibiting a composition evolution of the precursor powder from a mixture of $LiAc{\cdot}2H_2O$, $LaAc_3{\cdot}1.5H_2O$, and TiO_2 to pure phase lithium lanthanum titanate with increasing temperature. It can be seen from Fig. 2(b) that the sample annealed at 450 °C presents strong peaks arising from lanthanum oxide and lanthanum titanium oxide, indicating the complete decomposition of lanthanum acetate and the emergence of a compound reaction between the titanium and lanthanum oxides at this temperature. It also reveals that the 2nd weight loss in the TGA plot (shown in Fig. S1, ESI†) is

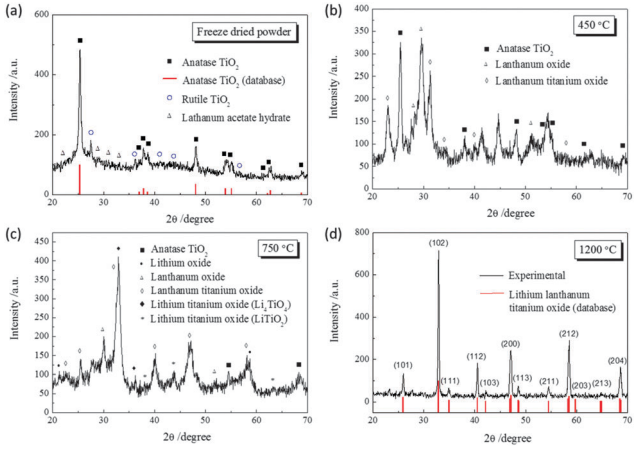

Fig. 2 XRD patterns of (a) freeze dried powder, and (b)–(d) powder annealed at 450 °C, 750 °C, and 1200 °C, respectively.

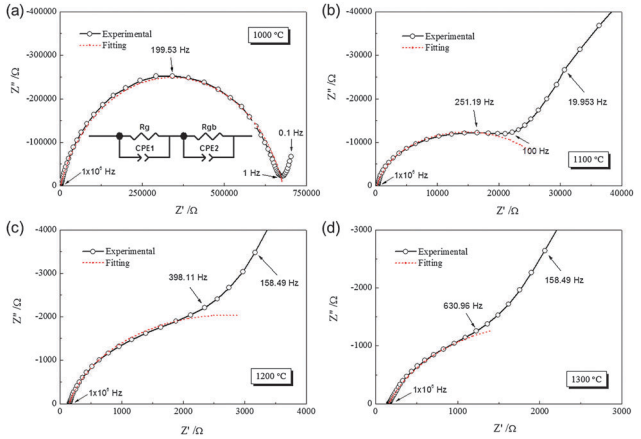

Fig. 3 Impedance spectra of $Li_{0.3}La_{0.57}TiO_3$ sintered at (a) 1000 °C, (b) 1100 °C, (c) 1200 °C, and (d) 1300 °C marked with representative values of the applied frequency. The inset of (a) depicts the equivalent circuit employed for fitting the impedance spectra (R_g: grain resistance, R_{gb}: grain boundary resistance, CPE: constant phase element.)

due primarily to the decomposition of lanthanum acetate. The decomposition of lithium acetate occurs at relatively high temperature as evidenced by the XRD analysis shown in Fig. 2(c), which corresponds to the sample annealed at 750 °C and presents the peaks of lithium oxide and lithium titanium oxides in addition to those of lanthanum oxide and lanthanum titanium oxide. Considering both the XRD and TGA results, it is clear that a major weight loss of the precursor powder mainly involving the decomposition of lithium and lanthanum acetates takes place when the annealing temperature reaches 750 °C. This confirms the rationality of the 750 °C temperature adopted for the pre-heat treatment of the precursor powder prior to making the pellets. Note that such a pre-heat treatment of the precursor powder with the use of appropriate temperature is a critical step to avoid the pellets from collapsing as a result of a too big volume change during the sintering. From the XRD pattern shown in Fig. 2d, it can be seen that, when being annealed at 1200 °C, the precursor material converts to nearly pure phase lithium lanthanum titanate, implying that the as-described coagulated solution method is an effective way to synthesize ternary oxides with a well-controlled stoichiometric ratio.

The performance of the prepared $Li_{0.3}La_{0.57}TiO_3$ for lithium ion conduction was studied by measuring the impedance spectra of pellets made of the precursor powder pre-heated at 750 °C in the frequency range from 0.01 Hz to 1 MHz using an impedance analyzer (Model: Solartron 1260/1287) with 10 mV ac amplitude at room temperature. The pellets were prepared using a cold pressing method at 130 MPa pressure and were then sintered at certain temperatures for 6 h in air. A Ti film of ~100 nm in thickness was deposited on both sides of the pellets to function as a blocking electrode for lithium ionic conductivity measurements. Shown in Fig. 3 are impedance spectra of the $Li_{0.3}La_{0.57}TiO_3$ samples sintered at 1000, 1100, 1200 and 1300 °C. Table 1 summarizes the gain ionic conductivity and overall ionic conductivity of these four samples, which are obtained by fitting the measured impedance plots using the equivalent circuit shown in the inset of Fig. 3a. In the equivalent circuit, R_g and R_{gb} represent the resistance corresponding to the ion conduction inside the grains and the resistance arising from the ion conduction at grain boundaries, respectively.[38–45] The lithium ionic conductivity, σ, was calculated using the formula $\sigma = d/(A \cdot R)$, where d is the pellet thickness, A is the area of metal electrodes, and R is the value of resistance obtained from fitting the impedance spectrum. The grain conductivity and overall conductivity were calculated using the grain resistance, R_g, and the overall resistance, $R_g + R_{gb}$, respectively.

Table 1 A summary of grain conductivity and overall conductivity of the $Li_{0.3}La_{0.57}TiO_3$ sintered at 1000, 1100, 1200 and 1300 °C

Sample No.	Sintering temperature (°C)	Grain conductivity (S cm^{-1})	Overall conductivity (S cm^{-1})
1	1000	4.75×10^{-5}	1.06×10^{-7}
2	1100	2.96×10^{-4}	2.30×10^{-6}
3	1200	3.03×10^{-4}	8.52×10^{-6}
4	1300	3.67×10^{-4}	1.52×10^{-5}

From the results listed in Table 1, one can see that the grain conductivity is on the order of 10^{-5} S cm^{-1} for the sample sintered at 1000 °C, and it increases by more than six times to the order of 10^{-4} S cm^{-1} when the sintering temperature reaches 1100 °C, implying the formation of pure phase lithium lanthanum titanate approximately at this temperature. A further increase of the sintering temperature to even 1300 °C shows no significant contribution to improving the grain conductivity. As for the overall conductivity, a considerable increase of the overall conductivity from 1.06×10^{-7} S cm^{-1} to 2.30×10^{-6} S cm^{-1} is observed when the sintering temperature increases from 1000 °C to 1100 °C. This can be attributed to an increase in the grain size and improved connection between individual grains due to the melt of material at elevated temperatures, being consistent with the SEM images shown in Fig. 4, which reveal that (1) the grains grow from ~500–800 nm (Fig. 4a) to averagely 2 μm (Fig. 4b) as the sintering temperature increases from 1000 °C to 1100 °C, and (2) the voids existing between the grains are largely reduced in view of the melt of the material at the temperature around 1100 °C. As the sintering temperature increases from 1100 °C to 1200 °C, and then to 1300 °C, the overall conductivity displays a gradual increase, from 2.30×10^{-6} S cm^{-1} to 8.52×10^{-6} S cm^{-1} and 1.52×10^{-5} S cm^{-1}, respectively. The increase in the overall conductivity with increasing sintering temperature results from the continued growth of the grains, from ~2 μm for 1100 °C to larger than 5 μm for 1300 °C, and a further decrease of grain boundaries,

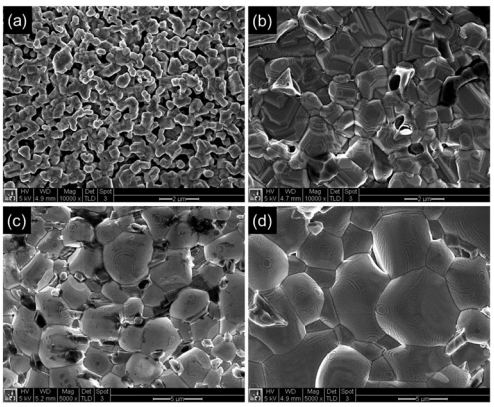

Fig. 4 SEM images of the $Li_{0.3}La_{0.57}TiO_3$ pellet samples sintered at (a) 1000 °C, (b) 1100 °C, (c) 1200 °C, and (d) 1300 °C (Scale bar: 2 μm for (a) and (b), 5 μm for (c) and (d)).

as shown in Fig. 4b–d. These results, *i.e.*, the grain conductivity on the order of 10^{-4} S cm^{-1} and the overall conductivity on the order of 10^{-5} S cm^{-1} for the pellet sample sintered at 1300 °C, are comparable to most of the values and are slightly higher than some of the values of conductivities reported in literature for the $Li_{0.3}La_{0.57}TiO_3$ synthesized using the traditional solid state reaction method[16,18,27,35,46,47] or the sol–gel method,[31,32,48,49] which are typically on the order of 10^{-4}–10^{-3} S cm^{-1} for the grain conductivity and on the order of 10^{-6}–10^{-5} S cm^{-1} for the overall conductivity (note that in some reports a temperature even higher than 1300 °C was adopted for sintering). While the achieved conductivities are at the same level, compared with the traditional methods, our coagulated solution method in terms of material synthesis is however much simpler and highly efficient.

In summary, the coagulated solution method involving dissolving lithium acetate and lithium lanthanum and dispersing commercial TiO_2 nanoparticles in acetic acid has proven to be an effective approach for the preparation of $Li_{0.3}La_{0.57}TiO_3$ precursor powder, which gives rise to a highly homogeneous distribution of the component elements through a simple, scalable, and reproducible way. The lithium ionic conductivities of $Li_{0.3}La_{0.57}TiO_3$ produced using this method are on the order of 10^{-4} S cm^{-1} for single crystalline grains and 10^{-5} S cm^{-1} for the bulk material. The conductivities are comparable to the values reported in literature for the material synthesized using a solid state reaction or sol–gel method. In addition to the synthesis of $Li_{0.3}La_{0.57}TiO_3$, the coagulated solution method is also thought of as an extendable approach for the fabrication of other multi-element oxides with the capability to easily and consistently control the stoichiometric composition of the material.

This work is supported financially in part by Korea Atomic Energy Research Institute.

Notes and references

1 D. Doughty and E. Peter Roth, *Electrochem. Soc. Interface*, 2012, **21**, 37.
2 M. Park, X. Zhang, M. Chung, G. B. Less and A. M. Sastry, *J. Power Sources*, 2010, **195**, 7904–7929.
3 D. Aurbach, E. Zinigrad, Y. Cohen and H. Teller, *Solid State Ionics*, 2002, **148**, 405–416.
4 N. Williard, W. He, C. Hendricks and M. Pecht, *Energies*, 2013, **6**, 4682–4695.
5 M. Yoshio, R. J. Brodd and A. Kozawa, *Lithium-ion batteries: science and technologies*, Springer, 2009.
6 J. Christensen, P. Albertus, R. S. Sanchez-Carrera, T. Lohmann, B. Kozinsky, R. Liedtke, J. Ahmed and A. Kojic, *J. Electrochem. Soc.*, 2012, **159**, R1–R30.
7 G. Girishkumar, B. McCloskey, A. Luntz, S. Swanson and W. Wilcke, *J. Phys. Chem. Lett.*, 2010, **1**, 2193–2203.
8 M. Ogawa, K. Yoshida and K. Harada, *SEI Tech. Rev.*, 2012, 88–90.
9 M. Yang and J. Hou, *Membranes*, 2012, **2**, 367–383.
10 V. Thangadurai and W. Weppner, *Ionics*, 2006, **12**, 81–92.
11 A. Manuel Stephan, *Eur. Polym. J.*, 2006, **42**, 21–42.
12 F. Croce, G. Appetecchi, L. Persi and B. Scrosati, *Nature*, 1998, **394**, 456–458.
13 N. Kamaya, K. Homma, Y. Yamakawa, M. Hirayama, R. Kanno, M. Yonemura, T. Kamiyama, Y. Kato, S. Hama and K. Kawamoto, *Nat. Mater.*, 2011, **10**, 682–686.
14 X.-W. Zhang, C. Wang, A. J. Appleby and F. E. Little, *J. Power Sources*, 2002, **112**, 209–215.
15 J. Emery, J. Buzare, O. Bohnke and J. Fourquet, *Solid State Ionics*, 1997, **99**, 41–51.
16 Y. Inaguma, J. Yu, T. Katsumata and M. Itoh, *Nippon Seramikkusu Kyokai Gakujutsu Ronbunshi*, 1997, **105**, 548–550.
17 S. Stramare, V. Thangadurai and W. Weppner, *Chem. Mater.*, 2003, **15**, 3974–3990.
18 K.-Y. Yang, J.-W. Wang and K.-Z. Fung, *J. Alloys Compd.*, 2008, **458**, 415–424.
19 S. Duluard, A. Paillassa, L. Puech, P. Vinatier, V. Turq, P. Rozier, P. Lenormand, P.-L. Taberna, P. Simon and F. Ansart, *J. Eur. Ceram. Soc.*, 2013, **33**, 1145–1153.
20 M. Kotobuki, K. Hoshina, Y. Isshiki and K. Kanamura, *Phosphorus Res. Bull.*, 2011, **25**, 61–63.
21 D. Popovici, H. Nagai, S. Fujishima and J. Akedo, *J. Am. Ceram. Soc.*, 2011, **94**, 3847–3850.
22 E. J. Cussen, *J. Mater. Chem.*, 2010, **20**, 5167–5173.
23 V. Thangadurai, H. Kaack and W. J. Weppner, *J. Am. Ceram. Soc.*, 2003, **86**, 437–440.
24 V. Thangadurai and W. Weppner, *Adv. Funct. Mater.*, 2005, **15**, 107–112.
25 A. Hayashi and M. Tatsumisago, *Electron. Mater. Lett.*, 2012, **8**, 199–207.
26 A. Sakuda, A. Hayashi and M. Tatsumisago, *Sci. Rep.*, 2013, **3**, 2261.
27 C. W. Ban and G. M. Choi, *Solid State Ionics*, 2001, **140**, 285–292.
28 K. Kishida, M. Miyata, N. Wada, N. L. Okamoto, K. Tanaka, H. Inui, H. Koyama, T. Hattori, Y. Iriyama and Z. Ogumi, *J. Electron Microsc.*, 2007, **56**, 225–234.
29 L. Sun, K. Sun and S. Dillon, *Proc. SPIE*, 2011, **8035**, 803508.
30 H. Geng, A. Mei, Y. Lin and C. Nan, *Mater. Sci. Eng., B*, 2009, **164**, 91–95.
31 H. X. Geng, J. L. Lan, A. Mel, Y. H. Lin and C. W. Nan, *Electrochim. Acta*, 2011, **56**, 3406–3414.
32 T. N. H. Le, M. Roffat, Q. N. Pham, S. Kodjikian, O. Bohnke and C. Bohnke, *J. Sol–Gel Sci. Technol.*, 2008, **46**, 137–145.
33 I. C. Popovici, E. Chirila, V. Popescu, V. Ciupina and G. Prodan, *J. Mater. Sci.*, 2007, **42**, 3373–3377.
34 H. Geng, A. Mei, C. Dong, Y. Lin and C. Nan, *J. Alloys Compd.*, 2009, **481**, 555–558.
35 Y. Inaguma, C. Liquan, M. Itoh, T. Nakamura, T. Uchida, H. Ikuta and M. Wakihara, *Solid State Commun.*, 1993, **86**, 689–693.
36 J. Wolfenstine, J. Allen, J. Read, J. Sakamoto and G. Gonalez-Doncel, *J. Power Sources*, 2010, **195**, 4124–4128.
37 R. H. Petrucci, W. S. Harwood, G. Herring and J. Madura, *General chemistry: principles and modern applications*, Prentice Hall, Upper Saddle River, NJ, 1997.
38 A. e. A. Saif and P. Poopalan, *Phys. B*, 2011, **406**, 1283–1288.
39 Z. V. Mocanu, G. Apachitei, L. Padurariu, F. Tudorache, L. P. Curecheriu and L. Mitoseriu, *Eur. Phys. J.: Appl. Phys.*, 2011, **56**, 132.
40 J.-M. Winand and J. Depireux, *Europhys. Lett.*, 1989, **8**, 447.
41 S.-i. Furusawa, *Phys. Solid State Ionics*, 2006, 271–302.
42 M. Kotobuki, in *2nd International Conference on Electrical, Electronics and Civil Engineering (ICEECE'2012)*, Singapore, 2012, pp. 165–167.
43 M. Kotobuki, K. Kanamura, Y. Sato, K. Yamamoto and T. Yoshida, *J. Power Sources*, 2012, **199**, 346–349.
44 M. Kotobuki, K. Kanamura, Y. Sato and T. Yoshida, *J. Power Sources*, 2011, **196**, 7750–7754.
45 O. Bohnke, S. Ronchetti and D. Mazza, *Solid State Ionics*, 1999, **122**, 127–136.
46 L. Sun, K. Sun and S. Dillon, in *Proc. of SPIE*, International Society for Optics and Photonics, 2011, pp. 803508.
47 C. H. Chen and K. Amine, *Solid State Ionics*, 2001, **144**, 51–57.
48 K. Dokko, N. Akutagawa, Y. Isshiki, K. Hoshina and K. Kanamura, *Solid State Ionics*, 2005, **176**, 2345–2348.
49 S. Suda, H. Ishii and K. Kanamura, *in Materials Research Society Symposium Proceedings*, Cambridge Univ Press, 2003, pp. 57–62.

